The bioactivity and ion release of titanium-containing glass polyalkenoate cements for medical applications

A. W. Wren · N. M. Cummins · F. R. Laffir ·
S. P. Hudson · M. R. Towler

Abstract The ion release profiles and bioactivity of a series of Ti containing glass polyalkenoate cements. Characterization revealed each material to be amorphous with a T_g in the region of 650–660°C. The network connectivity decreased (1.83–1.35) with the addition of TiO_2 which was also evident with analysis by X-ray photoelectron spectroscopy. Ion release from cements were determined using atomic absorption spectroscopy for zinc (Zn^{2+}), calcium (Ca^{2+}), strontium (Sr^{2+}), Silica (Si^{4+}) and titanium (Ti^{4+}). Ions such as Zn^{2+} (0.1–2.0 mg/l), Ca^{2+} (2.0–8.3 mg/l,) Sr^{2+} (0.1–3.9 mg/l), and Si^{4+} (14–90 mg/l) were tested over 1–30 days. No Ti^{4+} release was detected. Simulated body fluid revealed a CaP surface layer on each cement while cell culture testing of cement liquid extracts with TW-Z (5 mol% TiO_2) produced the highest cell viability (161%) after 30 days. Direct contact testing of discs resulted in a decrease in cell viability of the each cement tested.

1 Introduction

Glass polyalkenoate cements (GPC) has generated considerable interest recently as potential materials for the replacement of bone. Bone augmentation is required in cases where it is compromised by for example, osteoporosis [1] and osteomyelitis [2]. Surgical procedures that require augmentation include total hip replacement [3] which utilizes bone cement to secure the bond between the metallic implant and the bone [4], Vertebroplasty and kyphoplasty where cements restore vertebral body height and offer mechanical stability [5, 6]. However, a number of problems exist with the gold standard PMMA based bone cements. They do not form a chemical bond with the surrounding bone [7, 8], and experience up to 7% volumetric shrinkage[9] upon setting which contributes to aseptic loosening and subsequently implant failure. A setting exotherm of up to 120°C can also damage surrounding tissues. Studies have determined that temperatures above 60°C results in permanent cessation of blood flow in the tissue [10] and that coagulation of proteins and thermal necrosis of bone cells begins at 56°C [11]. Leaching of monomers and the generation of free radicals during setting can also have a negative effect on surrounding tissues and immune response [12, 13]. Increasing the bioactivity of bone cements has generated considerable interest recently as PMMA based cements are typically described as being bioinert in vivo. Calcium phosphate cements exhibit a degree of bioactivity [14], however extended setting times [15, 16] and low mechanical properties [17] have limited their use in load-bearing orthopedic applications.

GPCs have a number of attractive properties relevant for orthopedics. They can chemically bond to both bone and surgical metals [18], and can be tailored to release beneficial quantities of ions which can have positive effects in vivo [18, 19]. In this work, a titanium (Ti) substituted GPC was formulated as Ti is commonly used in both medical and dental applications. It is used for metallic implant materials in orthopedics [3], for crown and bridges in

A. W. Wren (✉) · M. R. Towler
Inamori School of Engineering, Alfred University, Alfred,
NY 14802, USA
e-mail: wren@alfred.edu

N. M. Cummins · F. R. Laffir
Materials and Surface Science Institute, University of Limerick,
Limerick, Ireland

S. P. Hudson
Waterford Institute of Technology, Waterford, Ireland

dentistry [20] and also has oral-maxillofacial applications [21]. Ti-based materials are also known to form a CaP surface layer when immersed in simulated body fluids [22, 23]. The presence of this layer is reported to be a prerequisite to bone bonding [23], which is beneficial as it results in implant stabilization. Additional components of these Ti-GPCs include zinc (Zn), strontium (Sr) and calcium (Ca) which all have been reported in the literature to have positive metabolic effects on bone [24–28], in addition Zn has also been reported to impart an antibacterial nature to the material [29, 30]. Previous work on these cements has resulted in increasing the handling and mechanical properties compared to a Ti-free GPC of similar composition [31]. Characterization of the Ti-glass phase has also revealed that the addition of TiO_2 results in an increased concentration of Si–O–NBO species [32]. In relation to bioactivity, network modifying alkali and alkali earth cations in the glass can disrupt the continuity of the glass network due to the breaking of some of the Si–O–Si groups leading to the formation of Si–O–NBO species [33]. The presence of these Si–O–NBO groups favors the ion exchange process where dissolution of the soluble silica content results in the formation of a SiO_2 rich surface layer and consequently Si–OH groups, and also the release of cations from the glass surface [33].

This study expands on previous work on these cements that were found to have increased mechanical and handling properties compared to control cement (BT 101). This study determines the ion release profiles, the ion release rates effect on the cement structure, and the bioactive response in simulated body fluid (SBF) and cell culture.

2 Materials and methods

2.1 Glass synthesis

Four glass compositions were formulated for this study with the principal aim being to investigate the substitution of Si with Ti throughout the glass series. BT 101 was used as a control, and glasses denoted TW-X, TW-Y and TW-Z contain incremental concentrations of Ti at the expense of Si (Table 1). Glasses were prepared by weighing out

Table 1 Ti glass compositions

	BT 101	TW-X	TW-Y	TW-Z
SiO_2	0.480	0.464	0.448	0.430
TiO_2	0.000	0.016	0.032	0.050
ZnO	0.360	0.360	0.360	0.360
CaO	0.120	0.120	0.120	0.120
SrO	0.040	0.040	0.040	0.040

appropriate amounts of analytical grade reagents (Sigma-Aldrich, Dublin, Ireland) and ball milling (1 h). The mix was then oven dried (100°C, 1 h), fired (1500°C, 1 h) in a platinum crucible and shock quenched in water. The resulting frit was dried, ground and sieved to retrieve a glass powder with a maximum particle size of 45 μm.

2.2 Glass characterisation

2.2.1 X-ray diffraction (XRD)

Diffraction patterns were collected using a Philips Xpert MPD Pro 3040/60 X-ray Diffraction Unit (Philips, the Netherlands). Disc samples (32 mm × 3 mm) were prepared by pressing a selected glass powder (<45 μm) into a backing of ethyl cellulose (8 tonnes, 30 s). Samples were then placed on spring-back stainless steel holders with a 10 mm mask and were analysed using Cu Kα radiation. A generator voltage of 40 kV and a tube current of 35 mA were employed. Diffractograms were collected in the range $5° < 2\theta < 80°$, at a scan step size 0.0083° and a step time of 10 s. Any crystalline phases present were identified using joint committee for powder diffraction studies standard diffraction patterns.

2.2.2 Differential thermal analysis (DTA)

A combined differential thermal analyser-thermal gravimetric analyser (DTA-TGA) (Stanton Redcroft STA 1640, Rheometric Scientific, Epsom, UK) was used to measure the glass transition temperature (T_g) for both glasses. A heating rate of 10°C min^{-1} was employed using an air atmosphere with alumina in a matched platinum crucible as a reference. Sample measurements were carried out every 6 s between 30 and 1000°C.

2.2.3 Network connectivity

The network connectivity (NC) of the glasses was calculated with Eq. 1 using the molar compositions of the glass. Network connectivity calculations were performed assuming that titanium performs as a network former and also as a network modifier.

$$NC = \frac{No.\ BOs - No.\ NBOs}{Total\ No.\ Bridging\ Species} \qquad (1)$$

where NC = Network connectivity; BO = Bridging oxygens; and NBO = Non-Bridging oxygens.

2.2.4 X-ray photoelectron spectroscopy

X-ray photoelectron spectroscopy (XPS) was performed in a Kratos AXIS 165 spectrometer using monochromatic Al

Kα radiation (hυ = 1486.6 eV) and a constant pass energy of 20 eV. Glass rods with dimensions of 15 × 3 × 3 mm were produced from the melt and fractured under vacuum ($\sim 2 \times 10^{-8}$ torr) to create pristine surfaces with minimum contamination. Surface charging was minimised by flooding the surface with low energy electrons. The C 1 s peak of adventitious carbon at 284.8 eV was used as a charge reference to determine the binding energies. For peak fitting, a mixed Gaussian-Lorenzian function with a Shirely type background subtraction was used.

2.3 Cement preparation

Cements were prepared by thoroughly mixing the glass powders (<45 μm) with E11 polyacrylic acid (PAA-Mw 210,000 <90 μm, Advanced Healthcare Limited, Kent, UK) and sterile water on a glass plate. The cements were formulated at P:L ratio of 2:1.5 with 50 wt% additions of PAA, where 1 g of glass powder was mixed with 0.37 g PAA and 0.37 ml water. Complete mixing was undertaken within 20 s for each disc. Cement discs were made by placing the viscous cements in 8∅ × 2 mm split ring moulds, clamped between two polyethylene plates and allowed to set in an oven at 37°C for 1 h prior to use. Cements were used immediately after setting (for ion release, SBF testing and cell culture) with minimal exposure to air. Cements from each formulation were produced identically and in triplicate for each test.

2.4 Preparation of extracts

Approximately 50 g of each glass (BT 101, TW-X, TW-Y, TW-Z) was sterilized using γ-irradiation at 25 kGray (Isotron ltd, Mayo, Ireland) prior to forming cements. Tissue culture water (Sigma-Aldrich, Dublin, Ireland) was selected as the solvent to prepare liquid extracts for ion release, SBF testing and cell culture analysis. The calculated surface area of each cement sample was used to determine the volume of extract required using Eq. 2.

$$Vs = \frac{Sa}{10} \qquad (2)$$

where Vs = volume of extract used and Sa = exposed surface area of the cement disc.

For cytotoxicity analysis both cements and extracts were used for analysis. Cement samples ($n = 3$) were aseptically immersed in appropriate volumes of sterile tissue culture water and agitated at (37 ± 2°C) for 1, 7 and 30 days. For cytotoxicity testing 100 μl aliquots ($n = 3$) of extract were removed after each time period. Additionally cements were incubated in cell culture wells and tested after 24 h for direct contact testing.

Table 2 AAS operating parameters

	Zn	Sr	Na	Ca
Lamp current (mA)	5	10	5	10
Fuel	Acetylene	Acetylene	Acetylene	Acetylene
Support	Nitrous Oxide	Nitrous Oxide	Air	Nitrous Oxide
Wavelength (nm)	213.9	460.7	330.2	239.9

2.5 Ion release profiles

The zinc (Zn), strontium (Sr), silica (Si), calcium (Ca) and titanium (Ti) ion concentration of the water extracts that contained the cement discs for each formulation ($n = 3$), were determined over 1, 7 and 30 days, and were measured using an atomic absorption spectrometer (AAS) (Varian SpectrAA-44-400) and the conditions are listed in Table 2.

Standard solutions were used for calibration of the system. NaCl was added to Sr and Na while LaCl was added to Ca to inhibit ionization of these elements. Three measurements were taken from each aliquot in order to determine the mean concentration of each element for each incubation period.

2.6 Surface area determination

In order to determine changes in surface area of the cements over time the advanced surface area and porosimetry, ASAP 2010 System analyser (Micrometrics Instrument Corporation, Norcross, USA) was employed. Approximately 60 mg of each set cement disc ($n = 3$) used for the ion release study was analysed with the addition of a control disc (not immersed in water, t-0). So for each formulation the SA was tested at t-0, 1, 7 and 30 days. Specific surface area changes were conducted using the Brunauer–Emmett–Teller (BET) method.

2.7 Simulated body fluid trial

Simulated body fluid (SBF) was produced in accordance with the procedure outlined by Kokubo et al. [23]. The composition of SBF is outlined in Table 3. The reagents were dissolved in order, from reagent 1–9, in 500 ml of purified water using a magnetic stirrer. The solution was maintained at 36.5°C. 1 M-HCl was titrated to adjust the pH of the SBF to 7.4. Purified water was then used to adjust the volume of the solution up to 1 l. Cement discs ($n = 2$) were immersed in concentrations of SBF as determined by Eq. 2 and were subsequently stored in for 1, 7 and 30 days in an incubator at 37°C. A JOEL JSM-840 scanning electron microscope equipped with a Princeton Gamma Tech

Table 3 Composition of SBF

Order	Reagent	Required amount
1	NaCl	7.996 g
2	$NaHCO_3$	0.35 g
3	KCl	0.224 g
4	$K_2HPO_4 \cdot 3H_2O$	0.228 g
5	$MgCl_2 \cdot 6H_2O$	0.305 g
6	1 M-HCl	40 ml
7	$CaCl_2$	0.278 g
8	Na_2SO_4	0.071 g
9	$NH_2C(CH_2OH)_3$	6.057 g

(PGT) Energy Dispersive X-ray (EDX) system was used to obtain secondary electron images and carry out chemical analysis of the surface of cement discs. All EDX spectra were collected at 20 kV, using a beam current of 0.26 nA. Quantitative EDX converted the collected spectra into concentration data by using standard reference spectra obtained from pure elements under similar operating parameters.

2.8 In vitro assessment of cements and extracts

The established cell line L-929 (American Type Culture collection CCL 1 fibroblast, NCTC clone 929) was used in this study as required by ISO10993 part 5 [34]. Cells were maintained on a regular feeding regime in a cell culture incubator at 37°C/5% CO_2/95% air atmosphere. Cells were seeded into 24 well plates at a density of 10,000 cells per well and incubated for 24 h prior to testing with both extracts and cement discs. The culture media used was M199 media (Sigma-Aldrich, Ireland) supplemented with 10% foetal bovine serum (Sigma-Aldrich, Ireland) and 1% (2 mM) L-glutamine (Sigma-Aldrich, Ireland). The cytotoxicity of

cement extracts was evaluated using the Methyl Tetrazolium (MTT) assay in 24 well plates. Extracts (100 μl) of undiluted sample ($n = 3$) were added into wells containing L929 cells in culture medium (1 ml) after 1, 7 and 30 day exposure to cement discs. Also cement discs ($n = 3$) were placed in the plate wells and were tested after 24 h (direct contact). Each of the prepared plates was incubated for 24 h at 37°C/5% CO_2. The MTT assay was then added in an amount equal to 10% of the culture medium volume/well. The cultures were then re-incubated for a further 2 h (37°C/5% CO_2). Next, the cultures were removed from the incubator and the resultant formazan crystals were dissolved by adding an amount of MTT Solubilization Solution (10% Triton X-100 in acidic isopropanol (0.1 N HCl)) equal to the original culture medium volume. Once the crystals were fully dissolved, the absorbance was measured at a wavelength of 570 nm. Aliquots (100 μl) of tissue culture water were used as controls, and cells were assumed to have metabolic activities of 100%. Cement discs and extracts in media without cells were tested and found not to interfere with the MTT assay.

3 Results and discussion

The bioactive response of a series of Ti substituted GPCs was evaluated to expand previous work which described the glass phase characterization [32], mechanical properties and setting of these cements [31]. Initial testing was performed on the glass both before and after γ-sterilization. Characterization of the glass phase of this cement series was carried out using XRD, DTA and NC calculations and XPS. X-ray diffraction patterns are presented in Fig. 1.

From Fig. 1 it can be seen that each material was found to be amorphous (BT 101-TW-Z), both before and after γ-sterilization. DTA revealed that T_g for the control glass, (BT 101) was found to be 657°C (Fig. 2a). Little change in

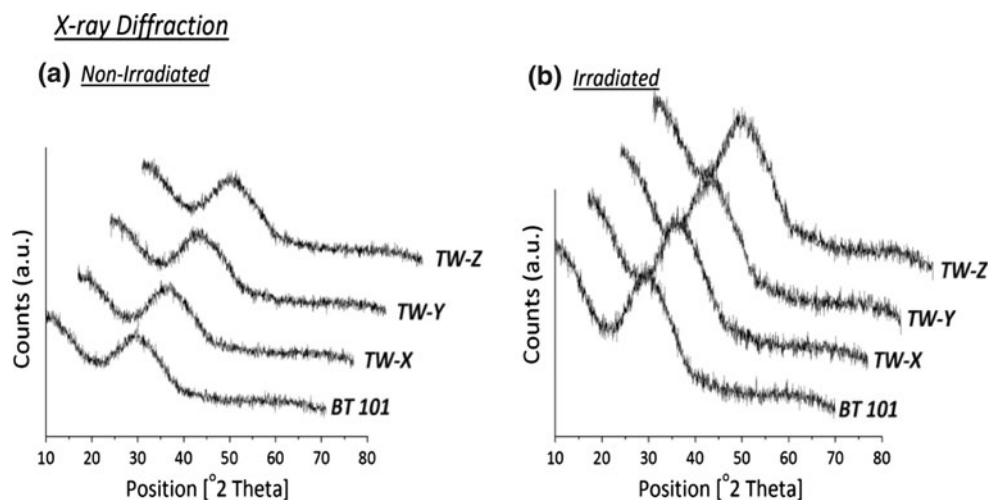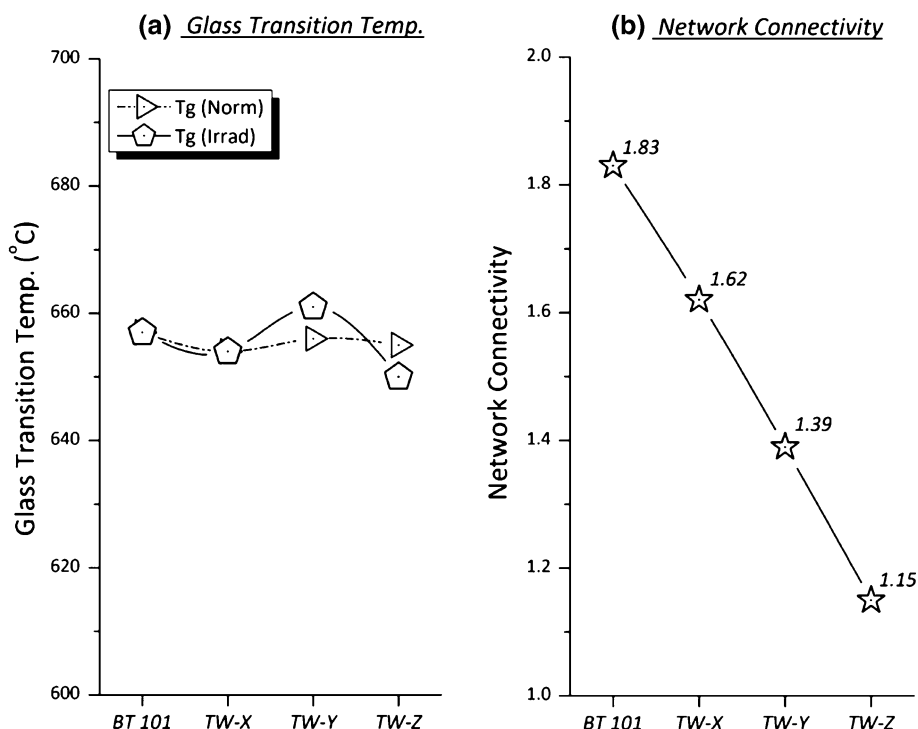**Fig. 1** XRD of **a** normal glass and **b** irradiated glass

Fig. 2 **a** Glass transition temperature of normal and irradiated glass. **b** Network connectivity of glass series

(a) *Glass Transition Temp.*

(b) *Network Connectivity*

T_g was found with the addition of up to 5 mol% TiO_2. TW-X, TW-Y and TW-Z were found to have a T_g of 654, 656 and 655°C respectively. γ-sterilization was also found to have little effect on the T_g of the glass series, where post-sterilization the T_g were 657, 654, 661 and 650°C for BT 101 TW-X, TW-Y and TW-Z respectively. This supports earlier studies on the effect of γ-sterilization on similar bioactive glasses where no structural changes were found [35].

The NC of the glass series was found to decrease from 1.83 to 1.69, 1.54 and 1.35 for BT 101, TW-X, TW-Y and TW-Z respectively, as the TiO_2 concentration in the glass increased (Fig. 2b). Previous work on similar glass compositions determined that Ti acted as a network modifier within the glass, where it forms sixfold octahedral groups resulting in an increase in the concentration of non-bridging oxygen (NBO) groups [32].

XPS was performed to distinguish between bridging (BO) and NBO. Figure 3a shows a high resolution O 1s spectrum from BT 101, while Fig. 3b shows O 1s from TW-Z. Asymmetry in the peak suggests the existence of two states for oxygen. Since the specimen glasses are cleaved in vacuum, the peak can be fitted with two component peaks at 530.6 and 531.9 eV to represent the NBO and BO respectively. Addition of TiO_2 in TW-Z, shifts the NBO peak to lower binding energy from 530.8 eV (BT101) to 530.6 eV and increases the ratio of NBO/BO from 1.2 to 1.9 as given in table in Fig. 3c. Peak fitting parameters and constraints are described elsewhere [32].

Previous studies determined that the dissolution and subsequent bioactivity of the glass surface is directly related to the concentration of NBO species. The addition of alkali and alkali earth cations (Na^+, K^+, Ca^{2+}) act as network modifiers that disrupt the continuity of the glassy network due to the breaking of some of the Si–O–Si bonds leading to the formation of Si–O–NBO [33]. In this study, peak shift in O 1s to lower binding energy and increased relative amount of NBO in TW-Z and in subsequent glasses with increasing TiO_2 content [32], is indicative of adding modifying cations to the glass. It is reported that the ion exchange process is favored by the presence of Si–O–NBO groups where the addition of alkali/alkali earth ions creates a larger number of these NBO groups in the glass structure leading to a higher dissolution rate of the silica [33].

Ion release profiles from each element from the cements were determined. It was found the Si, Zn, Ca, and Sr are being released from the cements. However, Ti is not being released or is released in levels below the detection limit of the instrument. The ion release profiles for the cements are presented in Fig. 4.

It can be seen from Fig. 4a that Si release levels reached approximately 14 mg/l at 1 day and comparisons between cements found there to be no significant difference. At 7 days, release levels reached 30–40 mg/l with significant change ($P = 0.014$) being evident between TW-Y (32 mg/l) and TW-Z (37 mg/l). After 30 days, Si release levels increased to within the region of 60–90 mg/l. BT 101 (61 mg/l) and TW-X (68 mg/l) showed no significant

Fig. 3 O 1s spectrum of **a** BT101, **b** TW-Z and **c** XPS data table

c.) XPS Data Table

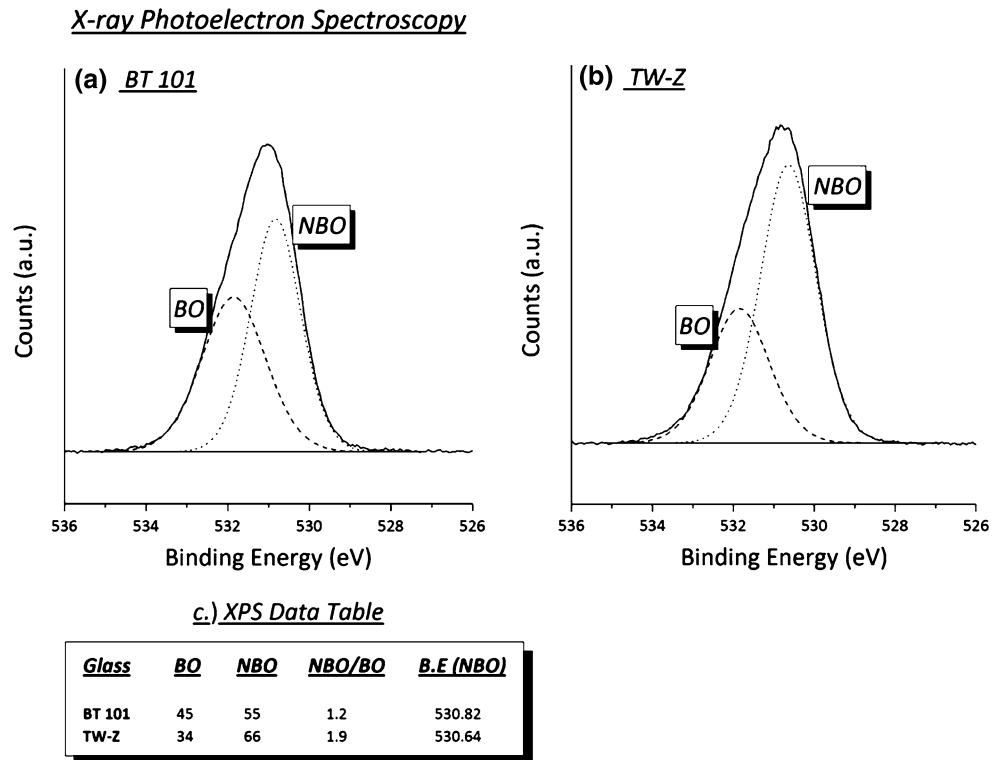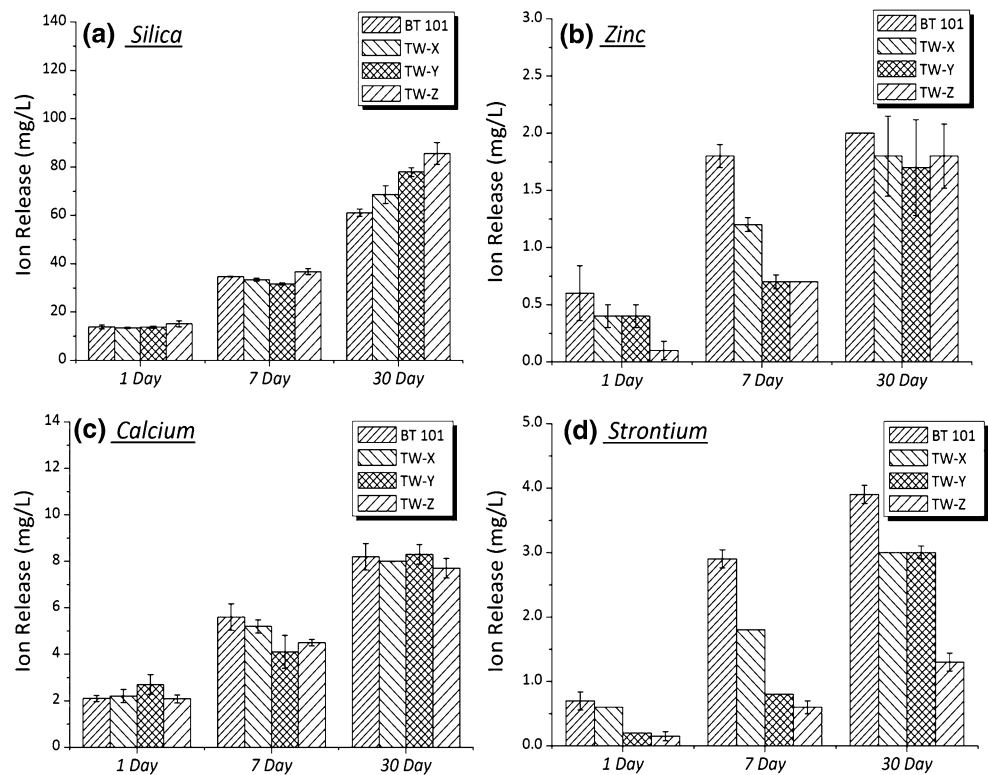| Glass	BO	NBO	NBO/BO	B.E (NBO)
BT 101	45	55	1.2	530.82
TW-Z	34	66	1.9	530.64

Fig. 4 Ion release profiles of **a** silica, **b** zinc, **c** calcium and **d** strontium

change, while both TW-Y (78 mg/l, $P = 0.034$) and TW-Z (86 mg/l, $P = 0.034$) showed a significant increase in Si release. This suggests the addition of Ti to the glasses facilitates an increase in the release of Si from the cements; however this only occurs after 30 days immersion in an aqueous medium. This may be attributed to Ti depolymerising the silicate network forming NBO species. The formation of NBOs in glasses is known to greatly contribute

to ion exchange and bioactivity [33]. It is also evident that each cement showed a cumulative increase in Si levels with respect to maturation particularly considering TW-Z were it increased from 15 mg/l to 37 mg/l ($P = 0.014$) between 1 and 7 days, and from 37 mg/l to 86 mg/l ($P = 0.001$) between 7 and 30 days. Figure 4b shows the Zn release rates over the same time period. Zn was found to be released in much lower levels than Si, ranging from 0.1–2.0 mg/l over 1–30 days. At 1 day, Zn release was found to reduce with the addition of Ti through the cement series. Zn levels significantly reduced ($P = 0.023$) from 0.6 mg/l (BT 101) to 0.1 mg/l (TW-Z). A similar trend was seen at 7 days where Zn reduced from 1.8 mg/l (BT 101) to 0.7 mg/l (TW-Z) ($P = 0.0001$). At 30 days the Zn levels increased in the Ti containing cements to similar levels presented by BT 101 (2.0 mg/l), no significant change was found between cements at this time period. However in a similar fashion to Si, the concentration of Zn was higher at each time interval as a result of the cumulative Zn release, particularly considering TW-Z were it increased from 0.1 to 0.7 mg/l ($P = 0.010$) between 1 and 7 days, and from 0.7 to 1.8 mg/l ($P = 0.011$) between 7 and 30 days.

From Fig. 4c it can be seen that Ca release showed relatively little change between each of the cements. Ca release levels ranged from 2.0 mg/l (TW-Z, 1 day) to 8.3 mg/l (TW-Y, 30 days). For each cement the Ca levels were found to be higher at each time interval. The most prominent increase in Ca release being for BT101 where Ca levels increased from 2.1 to 5.6 mg/l ($P = 0.015$) between 1 and 7 days, and from 5.6 to 8.2 mg/l ($P = 0.035$) between 7 and 30 days. Figure 4b shows the Sr release from the cements. Sr release ranged from 0.15 mg/l (TW-Z, 1 day) to 3.9 mg/l (BT 101, 30 days). It can be seen that the Sr release showed a general decrease when comparing BT 101 with the Ti containing cements. At 1 day the Sr release significantly decreased ($P = 0.013$) from 0.7 mg/l (BT 101) to 0.15 mg/l (TW-Z), at 7 days ($P = 0.0001$) 2.9 mg/l (BT 101) to 0.6 mg/l (TW-Z) and at 30 days ($P = 0.0001$) 3.9 mg/l (BT 101) to 1.3 mg/l (TW-Z). In a similar trend to each of the other ions, in each instance there was a higher concentration of ions detected at each time period, the most prevalent being with the control cement, BT 101. Sr levels increased from 0.7 to 2.9 mg/l ($P = 0.002$) between 1 and 7 days, and from 2.9 to 3.9 mg/l ($P = 0.017$) between 7 and 30 days. The decrease in the Sr release from the cement may be due to structures formed within the glass with the addition of Ti. Previous work on these glass formulations revealed that the Ti acts and a network modifying cation in the glass forming both tetrahedral (fourfold) and a number of octahedral (sixfold) structures. Excessive oxygen in octahedral structures requires charge compensation, which may be one possible explanation for the reduced Sr concentration with

the addition of Ti [32]. Overall cumulative ion release was found to be higher at each time period tested, however based on a daily release rate, ion release was found to reduce. This trend is valid as the cements structure matures and sets resulting in a lower solubility.

The surface area (SA) of each of the cements was determined using the BET method. BET was used in order to determine any changes in SA of the cements with exposure time in an aqueous environment, which will be related to the composition of the starting glass. Figure 5 shows the SA of the cements over 1 and 30 days.

Surface area measurements determined BT 101 to have an initial SA of 63 m^2/g which increased to 95 m^2/g at 1 day and was found to decrease to 24 m^2/g after 30 days. The Ti containing cements exhibited lower SA than BT 101, particularly in the case of TW-Z, where initially the SA was 48 m^2/g which increased slightly over 1 day (54 m^2/g) and 7 day (56 m^2/g) and reduced to 41 m^2/g after 30 days. However a general decrease in the SA can be observed with the increase in TiO_2 concentration. This is likely due to the open porosity, solubility and particulate composition of the set cements. A slight increase in the SA was observed in each of the cements after 1 day immersion in water. This is due to the dissolution of the PAA within the cement matrix resulting in open porosity, thus liberating ions bound within the cement structure. In the case of BT 101 it seems particle dissolution occurs at a greater extent and that it may be more soluble when compared to the Ti containing cements. This could be due to incomplete setting by a reduction in the concentration/formation of COO^-Ca^{2+}/Sr^{2+} polyacrylates. Previous work on these materials found that the Ti cements are more structurally stable when set than the Ti-free cement, BT 101, which is the likely reason for the reduced loss in SA as compared to BT 101 [31]. The higher concentration of NBO in the
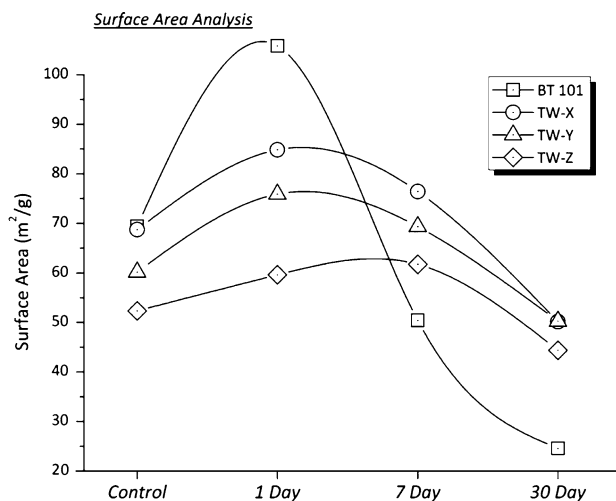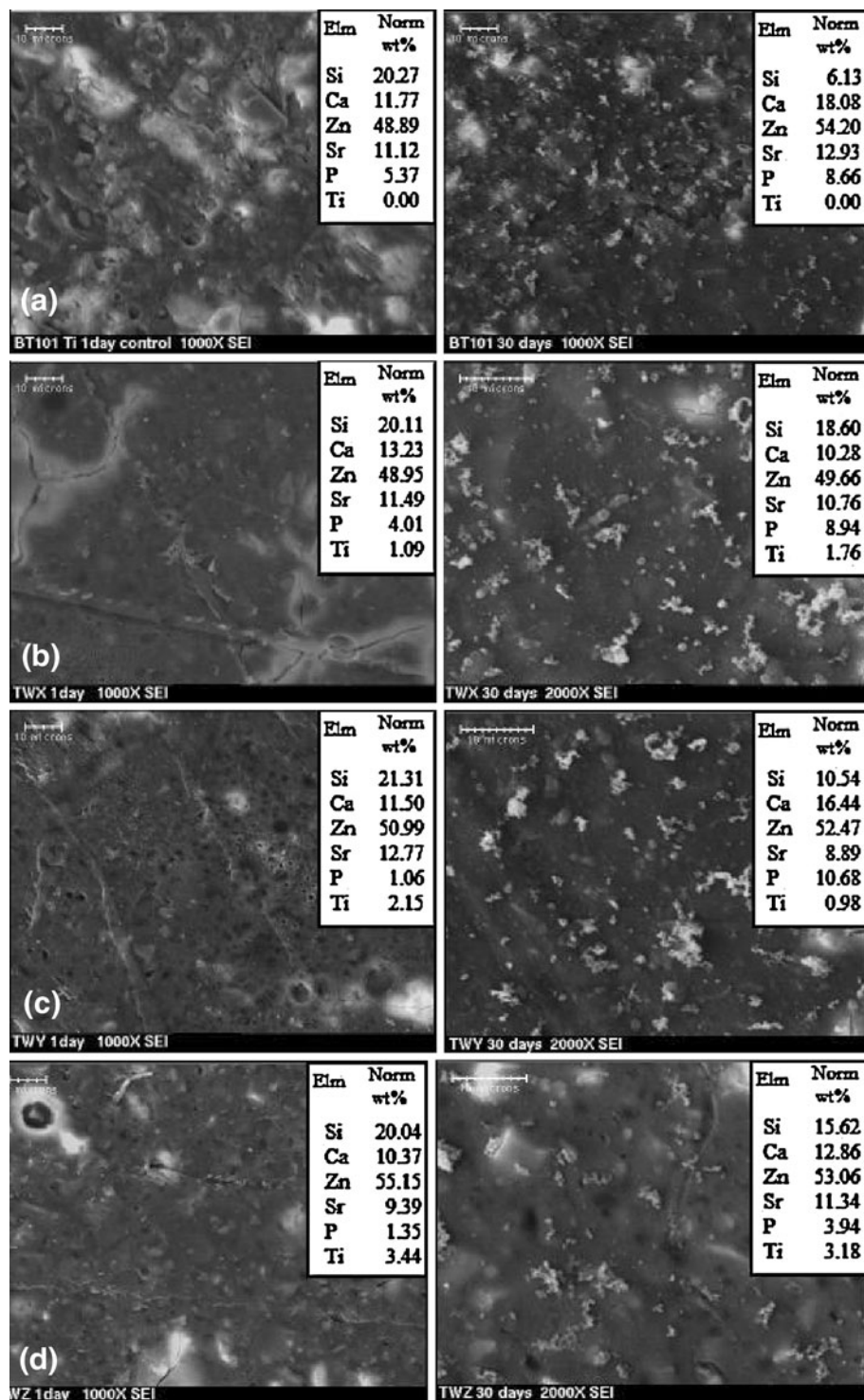

Fig. 5 Surface area of cements series as determined by ASAP

Fig. 6 SBF testing for **a** BT 101, **b** TW-X, **c** TW-Y and **d** TW-Z over 1–30 days

TW-Z glass phase will permit greater liberation of cations during the setting process which will subsequently facilitate a more matured set cement and resulting in less solubility. Form each of the Ti containing cements it can be seen that the surface area reduced as the Ti concentration increased, suggesting that the addition of Ti increases crosslinking within the cement, reducing solubility.

The bioactivity of the cements was determined using both simulated body fluid (SBF) and cell culture. SBF testing is used to determine a material's response in a physiological medium substitute. SBF was developed by Kokubo and Takadama as a synthetic form of blood plasma where it contains a similar ionic composition [36]. Precipitation of Ca^{2+} and PO_4^{2-} from this ionic solution to

form a CaP surface layer on the materials surface in SBF is seen as a precursor to bone bonding in vivo [37–39].

From Fig. 6 it can be seen that BT 101 exhibited a CaP surface layer (SEM & EDS) after 1 day, and increased up to 30 days. This trend can also be observed in each of the Ti containing cements (TW-X, TW-Y and TW-Z). It is likely that surface deposition occurs due to the presence of Ca and Si in the glass phase. The release of Ca^{2+} from the cements increases the Ca^{2+} concentration in the SBF and upon reaching the saturation limit, precipitation occurs and the negatively charged surface binds Ca^{2+} and PO_4^{2-}. The soluble silica content forms the negatively charged $Si-OH^-$ groups on the surface of the material [39, 40]. It is also evident that there is a high concentration of Zn^{2+} released from the cement which has previously been found to inhibit the crystallization of this surface layer to hydroxyapatite [41]. SBF testing revealed that surface precipitation of CaP was present on each of the cements at each time period.

Cell culture testing was performed using both cement discs and water based extracts released from the cements. For direct contact testing (Fig. 7a) it was found that there was a significant decrease in the viability of cells with each of the cements when compared to the control cells. BT 101 (2%, $P = 0.0001$), TW-X (1.2%, $P = 0.0001$), TW-Y (0.5%, $P = 0.0001$), TW-Z (0.4%, $P = 0.0001$). This is due to the gradual leaching of ions from the cements over 24 h into the enclosed environment of the cell culture wells. Ions leached from the cements (Ca^{2+}, Sr^{2+}, Zn^{2+}, Si^{2+}) quickly reach levels that are toxic to the cells resulting in a reduction in cell viability. There was found to be no significant change when comparing each of the cements.

Cement extracts were tested for cement over 1, 7 and 30 days. When comparing each of the cements to the control cells at 1 day, there was found to be no significant change in cell viability. A similar trend was observed at 7 days. At 30 days however both BT 101 (142%, $P = 0.001$) and TW-Z (161%, $P = 0.0001$) showed a significant increase in the cell viability. This suggests that solutions produced after 30 days are lower in toxicity, and are at levels favorable for cell proliferation. When considering the effect of maturation on each of the cements cell viability there was a general increase, however this only reached significance in a number of instances, BT 101 (1 and 30 days, $P = 0.020$) and TW-Z (1 and 30 days, $P = 0.0001$). Cell viability was found to increase with maturation time particularly with respect to BT 101 and TW-Z. Assuming cumulative ion release occurred for cement, it is possible that (since cell viability increased) the respective concentration of ions released is below the cells toxicity level or ions released from the cements aid in cellular metabolism.

The addition of Ti to Zn-GPCs has increased the fraction of NBO within the glass. This has resulted in an increase in Si release after 30 day, a reduction in Sr release and little change regarding Zn and Ca release. Cements containing Ti were also found to have a lower initial SA than the control cement; however this changed after 7 days, which suggests the Ti cements are less soluble or have a more defined set than the control material. CaP surface deposition was found on each of the cements at each time period tested. Cell culture testing revealed that TW-Z was found to have the highest cell viability than any other cement tested.

Fig. 7 Cell culture from cement extracts after 1, 7 and 30 days, and inset **a** Cement direct contact in cell culture

References

1. Kates SL, Kates OS, Mendelson DA. Advances in the medical management of osteoporosis. Injury. 2007;38S3:S17–23.
2. Henderson B, Nair SP. Hard labour: bacterial infection of the skeleton. Trends Microbiol. 2003;11(12):570–7.
3. Wise DL, Trantolo DJ, Lewandrowski KU, Gresser JD, Cattaneo MV, Yaszemski MJ. Biomaterials engineering and devices: human applications. Orthopaedic, dental and bone graft applications, vol. 2. Louisville: Humana Press; 2000.
4. Khan RJK, MacDowell A, Crossman P, Keene GS. Cemented or uncemented hemiarthroplasty for displaced intracapsular fractures of the hip—a systemic review. Injury. 2002;33:13–7.
5. Barrocas AM, Eskey CJ, Hirsch JA. Vertebral augmentation in osteoporotic fractures. Injury. 2007;38S3:S88–96.
6. Soin S, Kapural L, Mekhail N. Imaging for percutaneous vertebral augmenation. Tech Reg Anesth Pain Man. 2007;11:90–4.
7. Stanczyk M. Study on modelling of PMMA bone cement polymerisation. J Biomech. 2005;38(7):1397–403.
8. Donkerwolcke M, Burny F, Muster D. Tissues and bone adhesives—historical aspects. Biomaterials. 1998;19(16):1461–6.
9. Orr J, Dunne N. Measurement of shrinkage stresses in PMMA bone cement. Appl Mech Mater. 2004;1–2:127–32.
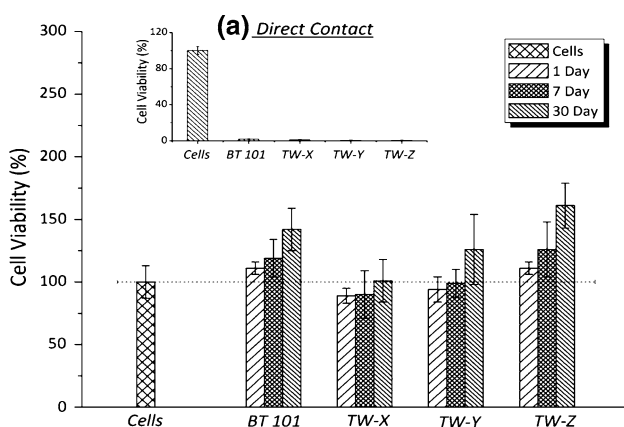10. Dunne NJ, Orr JF. Thermal characteristics of curing acrylic bone cement. ITBM-RBM. 2001;22(2):88–97.

11. Bergmann G, Graichen F, Rohlmann A, Verdonschot N, van Lenthe GH. Frictional heating of total hip implants. Part 2: finite element study. J Biomech. 2001;34(4):429–35.

12. Petty W. The effect of methyl methacrylate on chemotaxis of polymorphonuclear leukocytes. J Bone Joint Surg. 1978;60-A(4):493–7.

13. Santin M, Motta A, Borzachiello A. Effect of PMMA cement radical polymerization on the inflammatory response. J Mater Sci Mater Med. 2004;15:1175–80.

14. Ambard AJ, Mueninghoff L. Calcium phosphate cement: review of mechanical and biological properties. J Prosthodont. 2006;15(5):321–8.

15. Miyamoto Y, Ishikawa K, Takechi M, Toh T, Yoshida Y, Nagayama M, Kon M, Asaoka K. Tissue response to fast setting calcium phosphate cements in bone. J Biomed Mater Res. 1997;37(4):457–64.

16. Ishikawa K, Takagi S, Chow LC, Ishikawa Y. Properties and mechanisms of fast setting calcium phosphate cements. J Mater Sci Mater Med. 1995;6:528–33.

17. Bohner M. Physical and chemical aspects of calcium phosphates used in spinal surgery. Eur Spine J. 2001;10:S114–21.

18. Hatton PV, Hurrell-Gillingham K, Brook IM. Biocompatability of glass ionomer bone cements. J Dent. 2006;34:598–601.

19. DeBruyne MAA, DeMoor RJG. The use of glass ionomer cements in both conventional and surgical endodontics. Int Endod J. 2004;37:91–104.

20. Byon E, Moon S, Cho S-B, Jeong C-Y, Jeong Y, Sul Y-T. Electrochemical property and apatite formation of metal ion implanted titanium for medical implants. Surf Coat Technol. 2005;200(1–4):1018–21.

21. González JEG, Mirza-Rosca JC. Study of the corrosion behavior of titanium and some of its alloys for biomedical and dental implant applications. J Electroanal Chem. 1999;471(2):109–15.

22. Takadama H, Kim H-M, Kokubo T, Nakamura T. XPS study of the process of apatite formation on bioactive Ti-6Al-4 V alloy in simulated body fluid. Sci Technol Adv Mater. 2001;2:389–96.

23. Kokubo T, Kim H-M, Kawashita M. Novel bioactive materials with different mechanical properties. Biomaterials. 2003;24:2161–75.

24. Marie PJ. Strontium ranelate; a novel mode of action optimizing bone formation and resorption. Osteoporos Int. 2005;16:S7–10.

25. Marie PJ. Strontium ranelate: new insights into its dual mode of action. Bone. 2001;40(5):S5–8.

26. Yamaguchi M, Ma ZJ. Role of endogenous zinc in the enhancement of bone protein synthesis associated with bone growth of newborn rats. J Bone Miner Metab. 2001;19:38–44.

27. Yamaguchi M, Ma ZJ. Stimulatory effect of zinc on Deoxyribonucleic acid synthesis in bone growth of newborn rats:enhancement with zinc and insulin like growth factor-I. Calcif Tissue Int. 2001;69:158–63.

28. Devine A, Dick IM, Heal SJ, Criddle RA, Prince RL. A 4-year follow up study of the effects of calcium supplementation on bone density in elderly postmenopausal women. Osteoporos Int. 1997;7:23–8.

29. Wren AW, Boyd D, Thornton R, Cooney JC, Towler MR. Antibacterial properties of a tri-sodium citrate modified glass polyalkenoate cement. J Biomed Mater Res B Appl Biomater. 2009;90-B(2):700–9.

30. Sawai J. Quantative evaluation of antibacterial activities of metallic oxide powders (ZnO, MgO and CaO) by conductimetric assay. J Microbiol Methods. 2003;54:177–82.

31. Wren AW, Kidari A, Cummins NM, Towler MR. A spectroscopic investigation into the setting and mechanical properties of titanium containing glass ionomer cements. J Mater Sci Mater Med. 2010. doi: 10.1007/s10856-010-4089-2.

32. Wren AW, Laffir FR, Kidari A, Towler MR. The structural role of titanium in Ca-Sr-Zn-Si/Ti glasses for medical applications. J Non-Cryst Solids; 2010 (Submitted).

33. Serra J, Gonzalez P, Liste S, Chiussi S, Leon B, Perez-amor M, Ylanen HO, Hupa M. Influence of the non-bridging oxygen groups on the bioactivity of silicate glasses. J Mater Sci Mater Med. 2002;13:1221–5.

34. International Standard 10993-5, Biological evaluation of medical devices Part 5: tests for in vitro cytotoxicity. geneve, Switzerland; 1999.

35. Boyd D, Murphy S, Towler MR, Wren AW, Hayakawa S. Analysis of gamma-irradiated synthetic bone grafts by 29Si MAS-NMR spectroscopy, calorimetry and XRD. J Non-Cryst Solids. 2009;355(45–47):2285–8.

36. Kokubo T, Takadama H. How useful is SBF in predicting in vivo bone bioactivity. Biomaterials. 2006;27:2907–15.

37. Cho SB, Miyaji F, Kokubo T, Nakanishi K, Soga N, Nakamura T. Apatite formation on silica gel in simulated body fluid: effects of structural modification with solvent-exchange. J Mater Sci Mater Med. 1998;9:279–84.

38. Dong-Hui F, Zheng X, Shi-pu L, Yu-hua Y. Formation of apatite in simulated body fluid. J Wuhan Univ Tech-Mater Sci Ed. 2002;17(4):44–6.

39. Sun J, Li Y, Li L, Zhao W, Li L, Gao J, Ruan M, Shi J. Functionalization and bioactivity in vitro of mesoporous bioactive silicates. J Non-Cryst Solids. 2008;35S:3799–805.

40. Loof J, Svahn F, Jarmar T, Engqvist H, Pameijer CH. A comparative study of the bioactivity of three materials for dental applications. Dent Mater. 2008;24:653–9.

41. Boyd D, Towler MR, Wren AW, Clarkin OM, Tanner DA. TEM analysis of apatite surface layers observed on zinc based glass polyalkenoate cements. J Mater Sci. 2008;43:1170–3.